Civil Engineering Infrastructures Journal xx,xx
DOI: 10.22059/CEIJ.2024.361393.1932

Effect of Ferro-cement Confinement on Compressive and Splitting Tensile Behavior of Plain Concrete

Author 1:
Name: Abdullah-Al-Rafi
Affiliation: Undergraduate student, Department of Civil Engineering, Ahsanullah University of Science and Technology, Bangladesh.
Email: alrafiabdullah265@gmail.com
Mobile: +8801307266077

Author 2:
Name: Touhidul Islam
Affiliation: Undergraduate student, Department of Civil Engineering, Ahsanullah University of Science and Technology, Bangladesh.
Email: amtouhid9@gmail.com
Mobile: +8801710008966

Author 3:
Name: Kazi Rafid Ibtesham
Affiliation: Undergraduate student, Department of Civil Engineering, Ahsanullah University of Science and Technology, Bangladesh.
Email: kazirafid31@gmail.com
Mobile: +8801744957271

Author 4*:
Name: Debasish Sen
Affiliation: Assistant Professor, Department of Civil Engineering, Ahsanullah University of Science and Technology, Bangladesh.
Email: debasish.ce@aust.edu
Mobile: +8801724749478
ORCID No: 0000-0001-6375-4596

*Corresponding author: deebasish.ce@aust.edu

Received: 27/06/2023
Revised: 30/12/2023
Accepted: 12/02/2024

Abstract

This study aims to investigate the behavior of ferro-cement confined plain concrete (i.e., ultimate load, failure mechanism, damages, and ductility) under both compression and split tension. The main motivation of this study was the research gap concerning the split tensile behavior of ferro-cement confined concrete. In the experiment, ferro-cement confinement method (i.e., monolithic and non-monolithic casting of ferro-cement around concrete cylinders) and wire mesh content were the main variables. For each confinement method, ferro-cement with wire mesh contents of 0.22%, 0.25%, and 0.50% were considered. The test results demonstrated a notable capacity enhancement of concrete with ferro-cement confinement under both compression and split tension. In the test, cracks were originated and propagated radially from the outer ferro-cement shell towards the concrete core under compression, whereas cracks were generated and propagated in the opposite way under split tension. More damages, i.e., residual crack widths, were observed at the location of initial crack formation, irrespective of the parameters of this study, under both loadings. In addition, no distinct relationship was found between the displacement ductility and the parameters of this study.

Keywords: Strengthening, Performance, Retrofitting

1. Introduction

Concrete structures can deteriorate, which necessitates structural strengthening to achieve improved load-bearing capacity and durability. This structural strengthening involves the evaluation of the structure, identification of weaknesses, and implementation of a strengthening scheme on an existing building. Several strengthening schemes are available, including

additional structural member insertion and modification of structural elements using different materials (Bahmani and Zahrai, 2023). Common approaches include Fiber Reinforced Polymer (FRP) wrapping, concrete jacketing, Carbon Fiber Reinforced Polymer (CFRP), and Ferro-cement (FC) jacketing, etc. In the context of Bangladesh, where vulnerable buildings require attention, ferro-cement strengthening has a great prospect because of material availability, affordability, and strength enhancement potential. Ferro-cement strengthening of concrete may ensure upgraded structural performance, resilience, and safety of aging structures (Boban and John, 2021). Moreover, ferro-cement have also been utilized as a sustainable construction material (Minde et al., 2023). Therefore, several researchers investigated the effect of ferro-cement, as a strengthening material, on the behavior of structural elements, e.g., RC beams, columns, slab, panels, water tank, unreinforced masonry wall, etc. (Ahsan et al., 2023; El-Sayed et al., 2023a; Shaheen et al., 2023; Aules et al., 2022; Jaraullah et al., 2022; Amala et al., 2021; Erfan et al., 2021; Surendra and Ravindra, 2021). In addition, several researchers investigated the effect of ferro-cement on non-structural elements, e.g., masonry infill wall, water pipe, etc. (El-Sayed et al., 2023b; Sen et al., 2023). In this context, investigation of the behavior of plain concrete with ferro-cement confinement is important to properly understand the effect of ferro-cement on reinforced concrete. Previously, investigations on the ferro-cement strengthening technique of concrete cylinders were carried out by several researchers (i.e., Heng et al., 2017; Idris, 2016; Kaish et al., 2015; Xiong et al., 2011; Balaguru, 1989; Kaushik and Singh, 1997). Most researchers (Heng et al., 2017; Idris, 2016; Kaish et al., 2015; Balaguru, 1989) focused on the ferro-cement confinement of plain concrete only. However, few researchers (Xiong et al., 2011; Kaushik and Singh, 1997) focused on ferro-cement confined concrete cylinder specimens having longitudinal reinforcements.

Heng et al. (2017) investigated the behavior of ferro-cement confined concrete cylinders under axial compression. A 25 mm thick ferro-cement layer with either one, two, or three layers of wire mesh was cast around the concrete cylinders (100 mm in diameter and 200 mm in height). The wire mesh was a non-galvanized, expanded metal mesh with a diamond-shaped opening and a strand thickness of 0.84 mm. The experimental result showed 18–40% load capacity improvement, where no delamination of the ferro-cement layer was observed. Idris (2016) investigated different retrofitting methods, i.e., reinforced concrete confinement and ferro-cement overlay techniques for confining plain concrete cylinders (100 mm in diameter and 200 mm in height). Some concrete cylinders were retrofitted with an approximately 18-32 mm ferro-cement layer having either one or two layers of wire mesh (18-gauge woven wire mesh with a square opening of 12.5 mm). Ferro-cement retrofitted concrete cylinders exhibited 12–171% load capacity improvement under compression, where failure mode was reported as splitting for most of the retrofitted cylinders. Kaish et al. (2015) investigated the axial behavior of ferro-cement confined concrete of different sizes (diameters of 150, 100, and 75 mm). Each concrete cylinder was confined with a 12.5 mm ferro-cement layer having either single or double layers of welded wire mesh (with a square opening of 12.5 mm and a wire diameter of 0.85 mm). Ferro-cement jacketed concrete cylinders demonstrated a load capacity improvement of 13–48%, where vertical cracks were observed along the height of the ferro-cement layer. It is to be noted that disintegration of the ferro-cement layer and core concrete was observed in the case of ferro-cement confinement with a single-layer wire mesh. The displacement ductility (i.e., a ratio of displacement at 0.85 of the ultimate load on the post-peak stage to displacement at the yield load) of all jacketed cylinders was higher than that of non-jacketed cylinders. The displacement ductility varied between 1.34 and 2.43. Balaguru (1989) carried out an experimental investigation on concrete cylinders (150

mm in diameter and 300 mm in height) containing wire mesh layers. The main variables were concrete strength (i.e., 20 MPa and 40 MPa) and the number of layers of wire mesh (i.e., 2, 3, and 4 layers of wire mesh) in ferro-cement. The wire mesh was galvanized woven mesh with a square opening of 12.5 mm and a wire diameter of 1.09 mm. The experimental results showed an improvement in compressive strength of 11–33% and 18–30% (approximately) for normal and high-strength concrete, respectively, when wire mesh layers varied from 2–4 layers. The experimental observation showed that crack growth and crack network formation occurred in a much more controlled way in the case of the ferro-cement confined cylinders. The strain at peak compressive load was doubled by providing four layers of wire mesh in ferro-cement when compared to that of non-confined concrete cylinders. In summary, previous experimental studies on the ferro-cement strengthening of plain concrete mainly focused on the improvement of load-carrying capacity, the changes in ductility and/or displacement at peak strength, and the failure modes under compressive loading. However, load capacity improvement and failure mechanisms of ferro-cement confined concrete are not studied under split tensile loading, to the author's best knowledge. Since concrete is relatively weak under tension, a study is required to investigate the behavior of ferro-cement confined concrete under split tensile loads.

Therefore, the objective of this study is to comprehensively investigate the behavior of ferro-cement confined plain concrete under both compression and splitting tensile conditions. The investigated behavior includes ultimate load, failure mechanisms, damages, and displacement ductility.

2. Experimental Program

The experimental program includes two types of cylindrical specimens, i.e., unconfined and confined plain concrete, as shown in Figure 1. The unconfined specimens were cylinders of

100 mm diameter and 200 mm height. On the other hand, FC confined specimens had a 150 mm diameter, including a 25 mm FC shell, and a 200 mm height. A 25 mm mortar shell thickness, as suggested by Xiong et al. (2011) and Heng et al. (2017), was maintained at the outer edge of the core concrete. Two construction methodologies, namely, monolithic and non-monolithic casting, were adopted for FC shell construction. In monolithic construction, the core concrete and FC shell were constructed together. In contrast, the FC shell was constructed on hardened concrete in the case of non-monolithic construction.

Nine unconfined, i.e., control specimens were made, where a compression load test was conducted on five specimens and a split tensile test was conducted on four specimens following ASTM C 39/C 39M (2019) and ASTM C496 (2019), respectively. Meanwhile, six FC confined specimens were constructed for each volume fraction of wire mesh using both monolithic and non-monolithic casting methods. Among them, the compression load test was conducted on three specimens, and the split tensile test was conducted on three specimens. The configuration of all the specimens (unconfined and confined) is shown in Table 1.

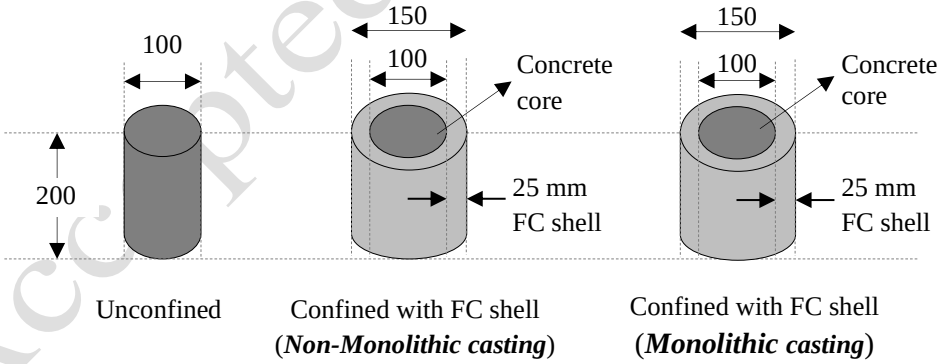

N.B.: Please refer to Figure 2 and 3 for Non-monolithic and Monolithic casting process

Fig. 1. Types of specimens in the current study (all dimensions are in "mm").

Table 1. Configuration of all types of specimens.

Specimen Type	Series name	Wire diameter (mm)	Wire spacing (mm)	Volume fraction, ρ (%)	No. of mesh layer, N	Shell thickness, t_s (mm)	Nominal diameter (mm)	Nominal height (mm)
Unconfined	C	-	-	-	-	-	100	200
Non-monolithically confined (RA)	RA_22	1.24	21.82	0.22	Single	25	150	200
	RA_25	1.02	12.8	0.25	Single	25	150	200
	RA_50	1.02	12.8	0.50	Double	25	150	200
Monolithically confined (RB)	RB_22	1.24	21.82	0.22	Single	25	150	200
	RB_25	1.02	12.8	0.25	Single	25	150	200
	RB_50	1.02	12.8	0.50	Double	25	150	200

2.1. Materials and Mix Design

The cement utilized in this study meets BDS EN 197-1, 2003 standards and can be classified as CEM-II/B-M. As per specification, the used cement is Portland Composite Cement (PCC), which contains clinker (65–69%), blast furnace slag, pulverized fuel ash/limestone-slag (31–35%), and gypsum (0–5%). The chemical composition of the clinker in the cement utilized in ferro-cement is given in Table 2. In concrete, 19 mm downgraded brick chips were used as coarse aggregate, and locally available river sand was used as fine aggregate. The material properties of the aggregates are given in Table 3. The concrete mix ratio was kept 1:2:4 (C: FA: CA) by volume, corresponding to M15 grade, with a water-cement ratio of 0.81. For the outer shell mortar, the mortar mix ratio was kept at 1:2.5 (C: FA) by weight, and the water-cement ratio ranged from 0.64 to 0.75. Tap water was used during the mixing of constituent materials of concrete and mortar. The mix proportions of concrete and ferro-cement

mortar are given in Table 4. At 28 days, the average compressive strength of unconfined concrete cylindrical specimens was 6.73 MPa, while the mortar cube strength was 13.12 MPa. Two types of wire mesh, with different wire diameters and spacing, were used in this study to achieve the target volume fractions of mesh reinforcement. The wire diameter, spacing, and average ultimate tensile strength of Type-1 wire mesh were 1.02 mm, 12.8 mm, and 268.9 MPa, respectively. On the other hand, Type-2 wire mesh had a wire diameter of 1.24 mm, a spacing of 21.8 mm, and an average ultimate tensile strength of 334.5 MPa.

Table 2. Chemical composition of clinker.

Constituent	Composition (%)
CaO	66.35
SiO_2	22.23
Al_2O_3	5.48
Fe_2O_3	3.47
MgO	0.85
SO_3	0.20

Table 3. Material properties of the aggregates.

Aggregate	Fineness modulus	Absorption capacity (%)	Bulk sp. gravity (SSD)	Bulk sp. gravity (OD)	Apparent sp. gravity
Brick chips	3.3	23.6	1.8	1.5	2.3
River sand	1.4	5.0	2.3	2.2	2.5

Table 4. Mix proportion of concrete and ferro-cement mortar.

Specimen type	**Concrete (Kg/m^3)**			**Ferro-cement mortar (Kg/m^3)**	
	Cement	**CA [SSD]**	**FA [SSD]**	**Cement**	**FA [SSD]**
Unconfined				-	-

Non-monolithically confined (RA)	205.7	1028.6	657.1	571.4	1428.6
Monolithically confined (RB)				-	-

2.2 Construction of Test Specimens

In this study, two types of construction methods were adopted to construct the confined specimens: non-monolithic (RA) and monolithic (RB) casting methods. In the non-monolithic casting method, 100 mm x 200 mm plain concrete cylinders were initially prepared. After seven days, the hardened concrete was chipped off and inserted into a PVC mold along with a 125 mm diameter wire mesh ring. Then, the mortar was poured into the empty spaces around the plain hard concrete in such a way that a 25 mm thickness of mortar shell was maintained around the core concrete. The construction sequence of the non-monolithic casting is illustrated in Figure 2. On the other hand, the concrete was directly poured into a PVC mold containing a 125 mm wire mesh ring in the monolithic casting method. The space between the mold and wire mesh ring was properly filled with the mortar matrix of the utilized concrete. The construction sequence of the monolithic casting is illustrated in Figure 3. During specimen casting, in both methods, the wire mesh ring was tried to keep at the center of the 25 mm FC shell. Galvanized Iron (GI) wires were utilized to securely fasten the joints of the wire mesh ring, ensuring that its stability is maintained. It is to be noted that a 100 mm overlap of wire mesh was incorporated to prevent reinforcement debonding, which is suggested by Kaushik et al. (1987).

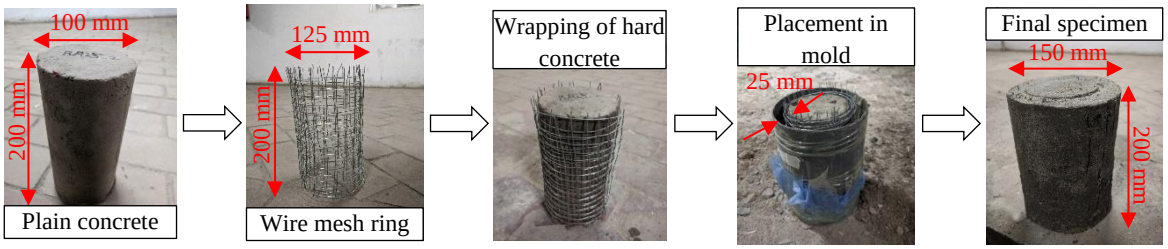

Fig. 2. Casting procedure of non-monolithically confined (RA) specimens.

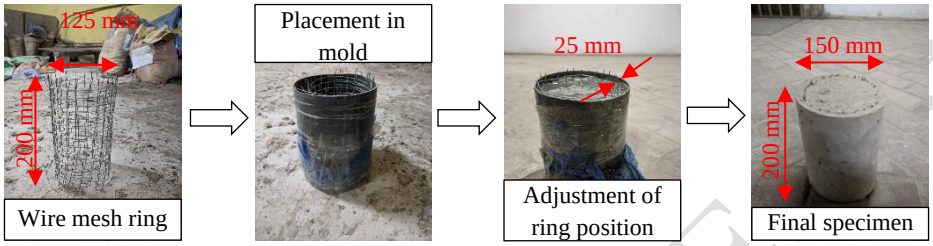

Fig. 3. Casting procedure of monolithically confined (RB) specimens.

3. Experimental Result and Discussion

3.1. Behavior Under Compression Load

The load-displacement relationship of both unconfined and confined specimens is depicted in Figure 4(a)–(b) for both non-monolithic and monolithic casting methods. The confined specimens demonstrated notably enhanced load-carrying capacity compared to the unconfined specimens. The experimental results showed that the compressive load capacity increased between 95 ~ 187% and 62 ~ 115% for monolithic and non-monolithic casting methods, respectively, when compared to unconfined concrete. The unconfined specimens experienced a sharp drop in load-carrying capacity, while the confined specimens exhibited a gradual decrease in load-carrying capacity. Specimen failure became apparent upon wire mesh rupture, accompanied by significant cracks on the mortar shell and a drop in load-carrying capacity.

Both unconfined and confined specimens showed vertical cracks on the outer side of the cylinder. Under the applied compressive load, the lateral expansion of the confined specimen's core concrete induced hoop tension in the ferro-cement shell due to Poisson's effect.

Consequently, this led to the expansion and subsequent cracking of the shell. Upon reaching the maximum compressive load, rapid increases in crack widths were observed. After examining the damaged specimens, common failure patterns were observed, as shown in Figure 5(a)–(b). For both non-monolithic and monolithic specimens, it was observed that cracks originated from the outer edge of the shell in a radial pattern and extended towards the core concrete. Additionally, multiple vertical cracks were observed on the FC shell. Similar failures were reported by other researchers, for instance, Idris (2016) and Kaish et al. (2015). Furthermore, crushing was observed at the top of the specimens. Nevertheless, there was more mortar spalling on the shell of monolithically cast specimens compared to non-monolithically cast specimens.

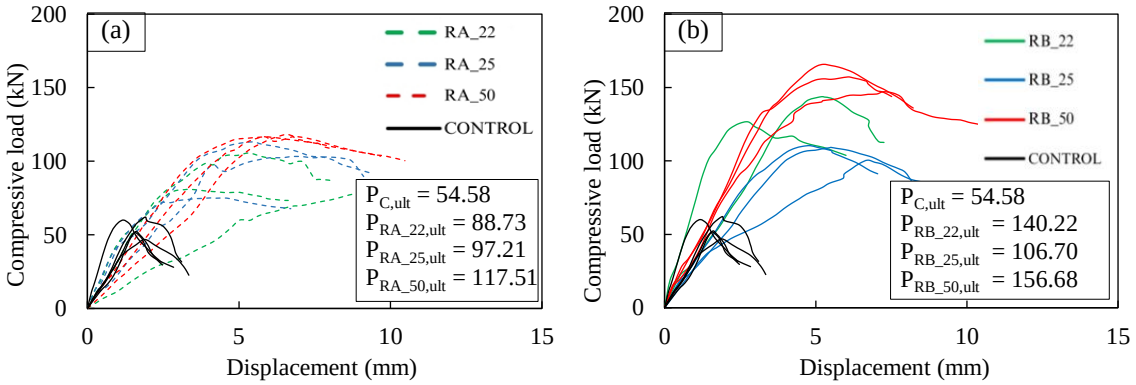

Fig. 4. Compressive load-displacement relationship of unconfined and ferro-cement confined specimens (a) non-monolithically confined and (b) monolithically confined.

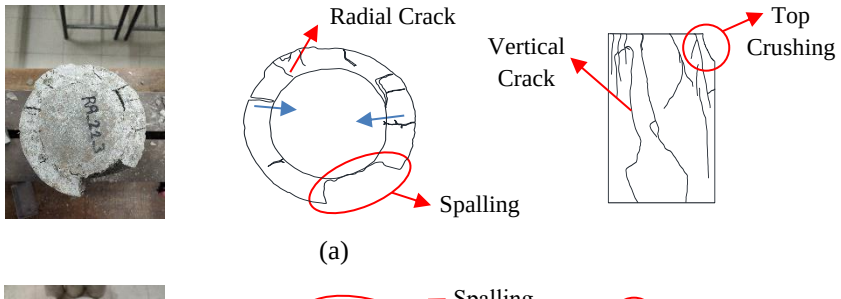

Fig. 5. Failure mode of (a) non-monolithic and (b) monolithic specimens under compressive load.

3.2. Behavior Under Split Tension

The experimental split tensile load capacity, and average crack width on the concrete core and the FC shell are presented in Table 5. The experimental results indicate that the split tensile load-carrying capacity increased between 68 ~ 212% and 80 ~ 101% for monolithic and non-monolithic casting methods, respectively, compared to unconfined concrete.

Both unconfined and confined specimens showed splitting failure. The split cracking originated from the core concrete and propagated towards the FC shell. This crack generation and propagation indicate that, at first, the core concrete failed under split tension, followed by cracking on the FC shell. Finally, the cracks in the core opened substantially, and loading was stopped. The rupture of the wire mesh was not observed. After examining the damaged confined specimens, common failure patterns were observed, as in Figure 6(a)–(b). It is to be noted that the split tensile behavior of ferro-cement confined plain concrete was found to be a research gap in the literature. Therefore, these results would be helpful in understanding the efficacy of ferro-cement to improve the concrete split tensile capacity and in understanding the corresponding crack propagation of ferro-cement confined concrete.

Table 5. Average experimental ultimate load and crack width of all specimens under split tension.

Specimen type	Series name	Average experimental ultimate load, P_{ult} (KN)	Average crack width (mm)	
			On core	On shell
Unconfined	C	30.84	2.01	-
Non-monolithically confined	RA_22	62.02	2.47	1.72
	RA_25	55.52	1.80	1.57
	RA_50	60.80	1.57	1.40
Monolithically confined	RB_22	69.06	7.00	1.45
	RB_25	51.82	5.50	1.10

	RB_50	96.34	3.83	0.87

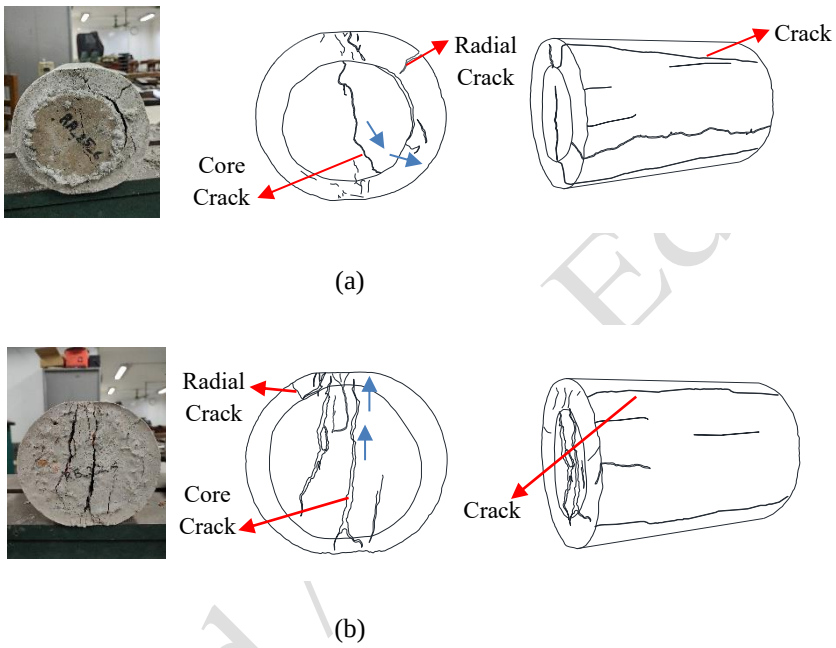

Fig. 6. Failure mode of (a) non-monolithic and (b) monolithic specimens under split tensile condition.

3.3. Effect of Different Parameters on the Performance of FC Confined Concrete

On compression and split tensile capacity

Figure 7(a) represents the compressive load capacities of all the specimens. For non-monolithic specimens (RA), compressive load capacity increased linearly with the increase in wire mesh content, i.e., volume fraction in the FC shell. In the case of monolithic specimens (RB), wire mesh confinement was effective in increasing the compressive load capacity; however, the relationship of capacity enhancement with the increase of wire mesh content in FC was not conclusive. In this context, a non-linear trend of compressive capacity improvement with an increasing number of wire mesh layers was evident in other previous studies (e.g.,

Balaguru, 1989; Idris, 2016). In contrast, a linear trend was also found by Kaish et al. (2015) based on only two ferro-cement confined cylinders having one and two layers of wire mesh in the ferro-cement. Nonetheless, the monolithically confined (RB) specimens exhibited a relatively higher load-carrying capacity in comparison to the non-monolithically confined (RA) specimens.

Figure 7(b) represents the split tensile capacities of all the specimens. In the case of both non-monolithic specimens (RA) and monolithic specimens (RB), wire mesh confinement was effective in increasing the split tensile load capacity; however, capacity enhancement was not linearly varied with the volume fraction of wire mesh in FC. It is also evident that both non-monolithic (RA) and monolithic (RB) specimens exhibited comparable load-carrying capacity under split tension, except for specimens with a 0.50% volume fraction of wire mesh.

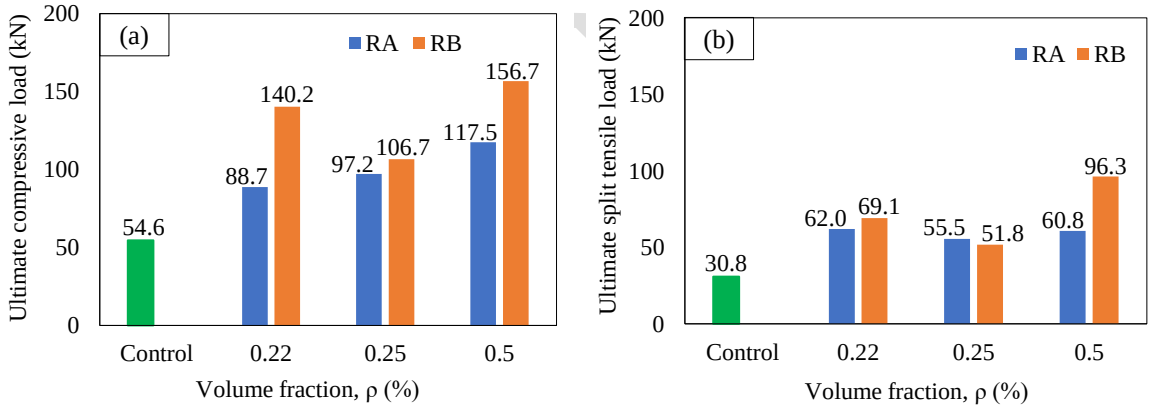

Fig. 7. Ultimate load capacity of unconfined and FC confined concrete under (a) compression and (b) split tensile condition.

On maximum residual crack width

The maximum residual crack width of all of the specimens was measured using a crack scale after the completion of each specimen test. Under the compression load, cracks originated at the FC shell and propagated towards the core concrete. The FC shell was cracked within a range of approximately 1.8 ~ 5.8 mm on average, whereas the concrete core was cracked within

a range of approximately 0.15 ~ 0.70 mm on average, which indicates that the FC shell was damaged more than the concrete core. The average core concrete crack width of all specimens under compression load is shown in Figure 8(a). The core concrete crack width decreased with the increase in wire mesh volume fraction in FC for both the non-monolithic and monolithic casting methods. Also, the residual crack widths were of similar order for both casting methods.

Under split tension, cracks initiated at the core concrete center and propagated towards the FC shell mortar. The FC shell was cracked within a range of approximately 0.9 ~ 1.7 mm on average, whereas the concrete core was cracked within a range of approximately 1.6 ~ 7.0 mm on average, which indicates that the concrete core was damaged more than the FC shell. The average FC shell crack width of all specimens under the split tensile load is shown in Figure 8(b). It is evident that the FC shell crack width decreased with the increase in wire mesh volume fraction in FC for both the non-monolithic and monolithic casting methods. Also, the residual crack widths were relatively lower for monolithic specimens.

In summary, the location of maximum damage varied under compression and split tension. However, under both loading conditions, more damages, i.e., residual crack widths, were observed at the location of initial crack formation, irrespective of the parameters of this study.

On displacement ductility

The displacement ductility was determined for specimens tested under compression loads as a ratio of displacement at 80% of the ultimate load after the post-peak and displacement at the maximum load. The average displacement ductility of all specimens (minimum 1.42 and maximum 1.76) under the compression load is shown in Figure 9. It is evident that wire mesh confinement marginally improved the ductility. In literature, Kaish et al. (2015) found displacement ductility (i.e., a ratio of displacement at 0.85 of the ultimate load on the post-peak

stage to displacement at the yield load) of all jacketed cylinders within a range of 1.34 to 2.43. The variation in the ranges of displacement ductility could be attributed to the differences between the definition of displacement ductility in this study and Kaish et al. (2015). Nevertheless, no remarkable relationship among displacement ductility, volume fraction of wire mesh in FC, and construction method was found in this study.

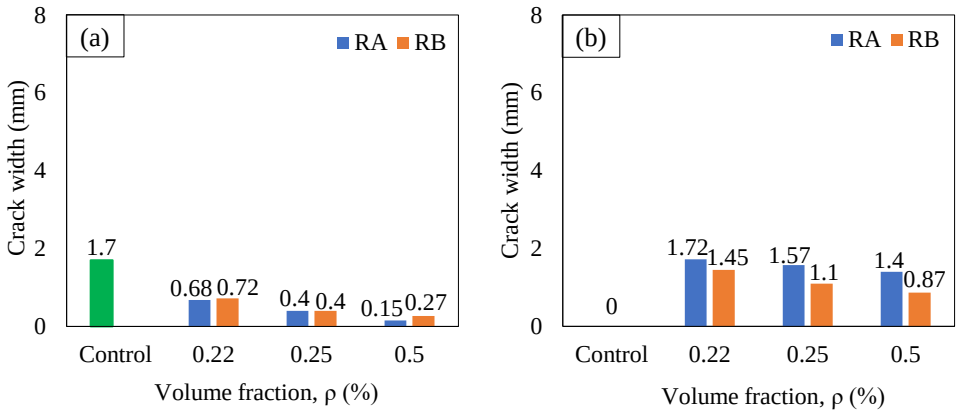

Fig. 8. Maximum crack width of (a) core concrete under compression and (b) FC shell under split tension.

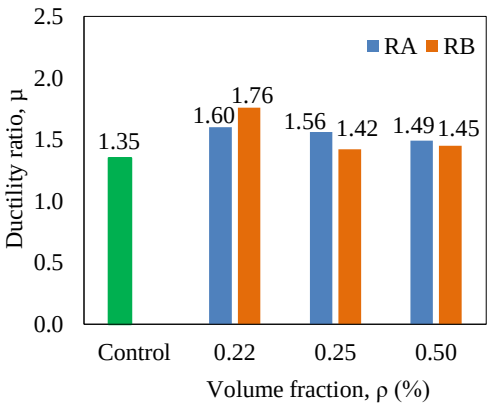

Fig. 9. Displacement ductility under compression load.

4. Conclusion

This study focused on the experimental behavior of unconfined and ferro-cement (FC) confined plain concrete cylinders under compression and split tension. Two construction methodologies, namely, non-monolithic and monolithic casting, were adopted for ferro-cement confinement.

In addition, 0.22%, 0.25%, and 0.50% volume fractions of wire mesh in ferro-cement were considered for each construction method. The following conclusions were drawn within the limited scope of this study:

- Compression load carrying capacity improved by 62% to 115% for non-monolithic specimens and 95% to 187% for monolithic specimens, with an increase in wire mesh volume fraction from 0.22% to 0.50%.
- Split tensile load capacity increased by 80% to 101% for non-monolithic specimens and 68% to 212% for monolithic specimens, with an increase in wire mesh volume fraction from 0.22% to 0.50%.
- Under compression, cracks originated from the outer edge of the ferro-cement shell in a radial pattern and extended towards the core concrete, irrespective of the parameters of this study. Whereas cracks originated at the center of core concrete and propagated radially towards the ferro-cement shell under split tensile load.
- The location of maximum damage varied under compression and split tension. However, under both loading conditions, more damages, i.e., residual crack widths, were observed at the location of initial crack formation, irrespective of the parameters of this study.
- No notable relationship among displacement ductility, volume fraction of wire mesh in ferro-cement, and construction method was found.

Conflicts of Interest

The authors have no conflicts of interest to declare.

References

Ahsan, R., Zahan, S., and Nahar, J. (2023). "Review of Tests on Ferrocement Retrofitted Unreinforced Masonry", *ACI Special Publication*, *358*, 179-205, https://doi.org/10.14359/51740236.

Amala, M., Dhal, L., Gokul, V., Christi, S., and Dhanasekar, K. (2021). "Strengthening of compression member by ferrocement with high performance mortar–Jacketing technique", *Materials Today: Proceedings*, *43*, 1810-1818, http://dx.doi.org/10.1016/j.matpr.2020.10.495.

ASTM C 39/C 39M (2019). "*Standard Test Method for Compressive Strength of Cylindrical Concrete Specimens"*, American Society for Testing and Materials (ASTM), USA.

ASTM C496 (2019). "*Standard Test Method for Splitting Tensile Strength of Cylindrical Concrete Specimens"*, American Society for Testing and Materials (ASTM), USA.

Aules, W. A., Saeed, Y. M., Al-Azzawi, H., and Rad, F. N. (2022). "Experimental investigation on short concrete columns laterally strengthened with ferrocement and CFRP", *Case Studies in Construction Materials*, *16*, e01130, https://doi.org/10.1016/j.cscm.2022.e01130.

Bahmani, M., and Zahrai, S. M. (2023). "Proposed Methodology and Comprehensive Design Process for Seismic Rehabilitation of Steel Structures with Supplemental Viscous Dampers", *Civil Engineering Infrastructures Journal*, *56*(1), https://doi.org/10.22059/CEIJ.2022.330808.1793.

Balaguru, P. (1989). "Use of ferrocement for confinement of concrete", *Journal of Ferrocement*, 19(2), 135-140.

BDS EN 197-1 (2003). "*Composition, specifications and conformity criteria for common cements"*, Bangladesh Standards and Testing Institution (BSTI), Bangladesh.

Boban, J. M., and John, A. S. (2021). "A review on the use of ferrocement with stainless steel mesh as a rehabilitation technique", *Materials Today: Proceedings*, *42*, 1100-1105, http://dx.doi.org/10.1016/j.matpr.2020.12.490.

El-Sayed, T. A., Shaheen, Y. B., Mohamed, F. H., and Abdelnaby, R. M. (2023a). "Performance of Ferrocement Composites Circular Tanks as a New Approach for RC Tanks", *Case Studies in Construction Materials*, 19, e02228, https://doi.org/10.1016/j.cscm.2023.e02228.

El-Sayed, T. A., Shaheen, Y. B., AbouBakr, M. M., and Abdelnaby, R. M. (2023b). "Behavior of ferrocement water pipes as an alternative solution for steel water pipes", *Case Studies in Construction Materials, 18,* e01806, https://doi.org/10.1016/j.cscm.2022.e01806.

Erfan, A. M., Abd Elnaby, R. M., Elhawary, A., and El-Sayed, T. A. (2021). "Improving the compressive behavior of RC walls reinforced with ferrocement composites under centric and eccentric loading", *Case Studies in Construction Materials, 14,* e00541, https://doi.org/10.1016/j.cscm.2021.e00541.

Heng, K., Areemit, N., and Chindaprasirt, P. (2017). "Behavior of concrete cylinders confined by a ferro-geopolymer jacket in axial compression", *Engineering and Applied Science Research,* 44(2), 90-96.

Idris, I. I. (2016). "Behavior and Strength of Concrete Cylinders Confined by Reinforced Concrete Jacket and Ferro Cement Overlay", *International Journal Science and Engineering Investigation,* 5(49):19-23.

Jaraullah, M. N. A., Dawood, E. T., and Abdullah, M. H. (2022). "Static and impact mechanical properties of ferrocement slabs produced from green mortar", *Case Studies in Construction Materials, 16,* e00995, https://doi.org/10.1016/j.cscm.2022.e00995.

Kaish, A. B. M. A., Jamil, M., Raman, S. N., and Zain, M. F. M. (2015). "Axial behavior of ferrocement confined cylindrical concrete specimens with different sizes", *Construction and Building Materials,* 78, 50-59, https://doi.org/10.1016/j.conbuildmat.2015.01.044.

Kaushik, S. K., Gupta, V.K. and Rahman, M.K. (1987). "Efficiency of mesh overlaps of ferrocement elements", *Journal of Ferrocement*.17, 329-36.

Kaushik, S., and Singh, S. (1997). "Behavior of ferrocement composite columns in compression", *ACI Special Publications,* 172, 669-682. https://doi.org/10.14359/6158.

Minde, P., Bhagat, D., Patil, M., and Kulkarni, M. (2023). "A state-of-the-art review of ferrocement as a sustainable construction material in the Indian context", *Materials Today: Proceedings,* https://doi.org/10.1016/j.matpr.2023.03.250.

Sen, D., Alwashali, H., Islam, M. S., Seki, M., and Maeda, M. (2023). "Lateral strength evaluation of ferrocement strengthened masonry infilled RC frame based on experimentally observed failure mechanisms", *Structures,* 58, p. 105428, https://doi.org/10.1016/j.istruc.2023.105428.

Shaheen, Y. B., Eltaly, B. A., Yousef, S. G., and Fayed, S. (2023). "Structural Performance of Ferrocement Beams Incorporating Longitudinal Hole Filled with Lightweight Concrete",

International Journal of Concrete Structures and Materials, *17*(1), 21, https://doi.org/10.1186/s40069-023-00579-3.

Surendra, B. V. and Ravindra, R. (2021). "A study of affordable roofing system using ferrocement and bamboo cement panels", *Journal of the Institution of Engineers (India): Series A*, *102*(3), 633-642, https://doi.org/10.1007/s40030-021-00533-0.

Xiong, G. J., Wu, X. Y., Li, F. F., and Yan, Z. (2011). "Load carrying capacity and ductility of circular concrete columns confined by ferrocement including steel bars" *Construction and Building Materials*, 25(5), 2263-2268, https://doi.org/10.1016/j.conbuildmat.2010.11.014.